ESS LINAC, DESIGN AND BEAM DYNAMICS

M. Eshraqi, H. Danared
European Spallation Source, Lund, Sweden

Abstract

The European Spallation Source, ESS, will use a linear accelerator delivering a high intensity proton beam with an average beam power of 5 MW to the target station at 2.5 GeV in long pulses of 2.86 ms. The ESS LINAC will use two types of superconducting cavities, spoke resonators at low energy and elliptical cavities at high energies. The possibilities to upgrade to a higher power LINAC at fixed energy are considered. This paper will present a review of the superconducting LINAC design and the beam dynamics studies.

INTRODUCTION

The European Spallation Source, ESS, to be built in Lund, Sweden, will require a high current proton LINAC to accelerate protons to be used for the spallation process on which high flux of pulsed neutrons will be generated. The accelerator is a 5 MW superconducting proton LINAC delivering beams of 2.5 GeV to the target in pulses of 2.86 ms long with a repetition rate of 14 Hz. Beam current is 50 mA, which at 352.21 MHz is equivalent to $\sim 9 \times 10^8$ protons per bunch. The latest design of the LINAC will be presented here and the 2003 Design Update can be found in table 1 and reference [1].

In this design it is foreseen not to exclude the possibility of a potential power upgrade of the LINAC. One of the scenarios for such a power upgrade would be increasing the power at the fixed energy of 2.5 GeV, by increasing the current.

SUPERCONDUCTING LINAC

The SC LINAC of ESS, blue part of Fig 1, starts from 50 MeV after a normalconducting LINAC, the orange part of Fig. 1, which is composed of a Low Energy Beam Transport, LEBT, a 352.21 MHz four-vane Radio Frequency Quadrupole, RFQ, a Medium Energy Beam Transport, MEBT, and a Drift Tube LINAC, DTL. The NC LINAC increases the energy from the ion source output, 75 keV, to 50 MeV.

Table 1: ESS main parameters

Parameter	Unit	2003 (LP/SP)*	2011
Ion	–	Proton / H^-	Proton
Energy	[GeV]	1.334	2.5
Beam power	[MW]	5.1	5
Repetition rate	[Hz]	$16\frac{2}{3}$ / 50	14
Beam current	[mA]	114	50
Beam pulse	[ms]	2 / 0.48	2.86
Duty cycle	[%]	3.3 / 4.8	4

* Long pulse / Short pulse.

Table 2: Parameters of the 2011 hybrid LINAC.

System	Energy MeV	Freq. MHz	β_{Geo}	No. of Md./Cv.*	Length m
Source	0.075	–	–	–	2.5
LEBT	0.075	–	–	–	1.6
RFQ	3	352.21	–	1	4.7
MEBT	3	352.21	–	2	1.0
DTL	50	352.21	–	3	19
Spokes	188	352.21	0.57	14 / 28	58
Low β	606	704.42	0.70	16 / 64	108
High β	2506	704.42	0.90	15 / 120	196

* Md. and Cv. represent the modules (RFQ tank, DTL tanks, cryo-modules) and the cavities, respectively.

The SC LINAC has two families of cavities, to name them, there is a family of double spoke resonators and two sets of five-cell elliptical cavities. The settings of the SC LINAC including the geometric β of the spoke resonators and elliptical cavities are found and reported in [2], for the sake of completeness they will be briefly mentioned here.

Spoke Resonators

Double spoke resonators are chosen for the energy range of 50 MeV to 188 MeV, for several reasons; their large transverse acceptance with respect to available normal conducting structures at this energy range and the ability to tune each cavity, being composed of just three gaps individually, which enhances their longitudinal acceptance during operation being two of the major ones.

Each cryomodule in the spoke region has two 352.21 MHz double spoke cavities, with a $\beta_{geo} = 0.57$ equivalent to a $\beta_{opt} = 0.50$, sandwiched between two superconducting quadrupoles, each 250 mm long. Neighboring cryomodules are separated by a utility module, 500 mm long, which houses the required diagnostics, and utilities, such as vacuum gauges, etc. There are 14 spoke cryomodules in the hybrid ESS LINAC.

Synchronous phase is set to $-20°$, and increases linearly to almost $-15°$ at the end of spokes, and the accelerating gradient stays fixed at 8 MV/m, except the first few periods

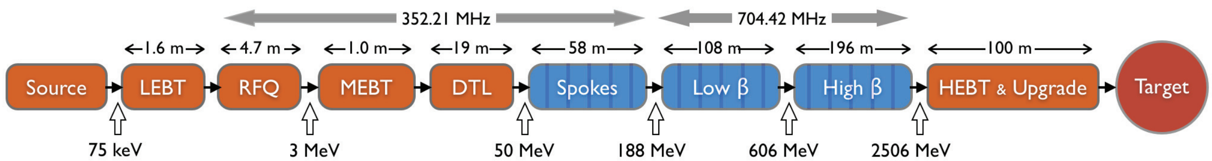

Figure 1: Block layout of the ESS hybrid LINAC 2011 (not to scale).

where the accelerating phase is lowered to have the same phase advance per meter as in the end of DTL.

Low β

To decrease the transverse size of the accelerator, and rf equipment, the rf frequency is doubled in the rest of the SC LINAC starting from the low beta cavities. To keep the acceptance constant in $Z - Z'$ phase space, the synchronous phase has to be lowered by a factor of two, and the accelerating field must be reduced by a factor of four [3]. On top of these the average longitudinal focusing force, phase advance per meter, should stay smooth and continuous. Therefore the synchronous phase starts at almost $-30°$ and asymptotically reaches $-15°$ at the end of low β section.

There are 16 low beta cryomodules and each of them is housing four five cell elliptical cavities sandwiched between two SC quadrupoles. The β_{geo} of the cavities is 0.70 and the quadrupole length is 400 mm. The accelerating gradient in this cavities is set to 15.44 MV/m [2], [4].

High β

The acceleration continues after 606 MeV using high β five-cell elliptical cavities, $\beta_{geo} = 0.90$. There are 15 high β cryo-modules each being composed of eight cavities and a pair of quadrupoles, one at each end of cryomodule. The synchronous phase stays at $-15°$, and the accelerating gradient is 18.17 MV/m.

BEAM DYNAMICS

To assure a good beam quality all along the LINAC and avoid losses and activations, all the known rules in designing a LINAC are taken into account in this design. To name them, zero current phase advance per period is always below 90° for the highly space charge dominated beam [6], however, for not to excite an envelope oscillation it is not equal to 60° [7]. The transverse to longitudinal phase advance ratio is chosen such that there is no emittance transfer from one plane to the other, Fig. 3 [8]. Last but not least, the phase advance per meter - average focusing force - varies smoothly and continuously.

Multiparticle beam dynamics simulations are performed using TRACEWIN [9], with 100,000 macroparticles with a Gaussian distribution in the 6D phase space, cut at $3 \times \sigma$. Initial beam emittance values are the output of 50 MeV DTL and the Twiss parameters are found by matching the beam

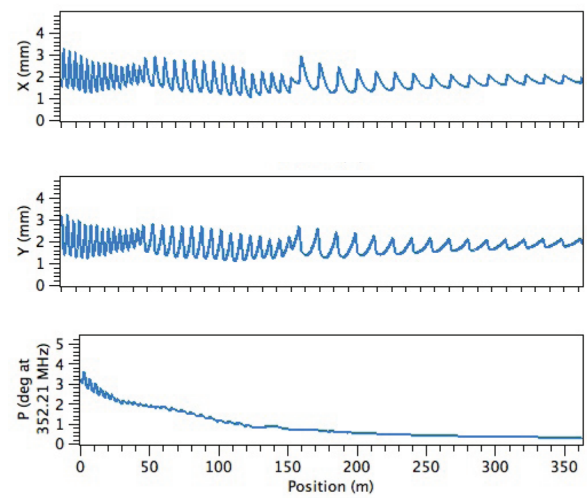

Figure 2: Beam rms sizes in three planes, Top: X, Middle: Y, Bottom: ϕ at 352.21 MHz.

to the SC LINAC. Matching between the structures is done by using a pair of quadrupoles, and a maximum of four cavities in each side of intersection. To have a current independent LINAC all matchings are done by smoothing the phase advance, not just adjusting the Twiss parameters. The rms envelopes of the beam along the LINAC are presented in Fig. 2. To improve the transition between DTL and spoke resonators, a single normal conducting quadrupole is added to the beginning of spokes, respecting the periodicity of the rest of the spokes.

Due to nonlinearity of the space charge forces in a Gaussian distribution, the beam reaches to a new equilibrium in the LINAC where the external focusing forces, quadrupole focusing, are linear. This redistribution of particles inside the beam is accompanied with a significant emittance growth in the first period, first row in Table 3. However, it has to be mentioned that a beam which is coming from DTL has already undergone this redistribution and will not suffer from this effect, as can be seen in the next rows of Table 3, also if a distribution like Kapchinskij-Vladimirskij (K-V) with linear space charge forces is used, the emittance growth due to redistribution is nullified. Lines with a negative emittance growth show where the ellipsoid rotates in the 6D phase space, causing its projection to reduce in one phase space and increase in another phase space.

The rms beam size stays within 3 mm of radius and the outermost particles do not exceed a radius of 12 mm. The resulted aperture to rms ratio in spoke region is almost 8

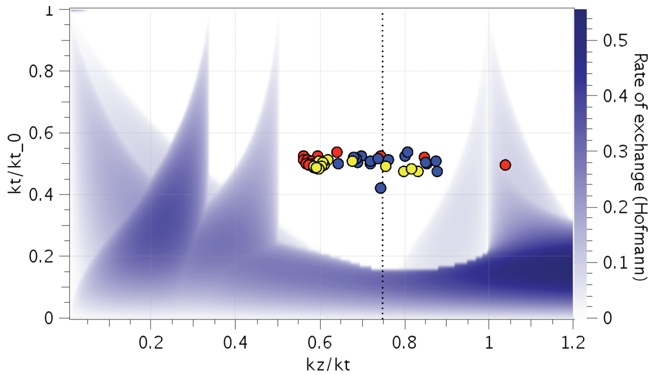

Figure 3: Working points of the SC LINAC on a Hofmann plot.

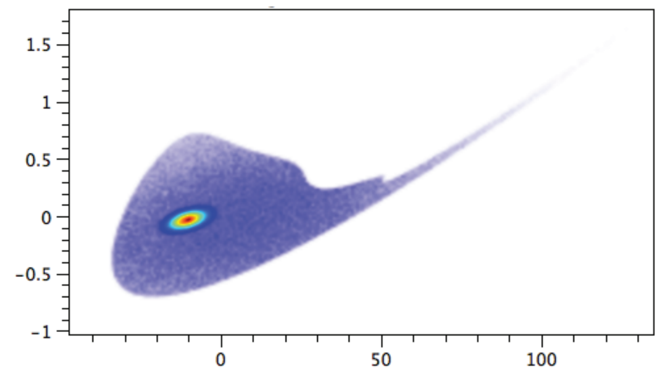

Figure 4: Acceptance (blue background) and the matched beam, E(MeV) vs. ϕ(deg) at 352.21 MHz at the injection to SC LINAC.

and it increases to 15 in the elliptical region. These ratios will decrease when errors are applied to the LINAC settings. However, an acceptance evaluation study indicated that the acceptance is one order of magnitude bigger than the beam in transverse planes, and is two orders of magnitude bigger in the longitudinal plane Fig. 4. To assess the sensitivity of different designs to initial mismatch and to compare them, the initial Twiss parameters are changed by $21, 69$, and 125% to achieve a mismatch of $10, 30$, and 50%, which caused an extra emittance increase of $4, 40$, and 90% respectively with respect to the nominal case. There are several combinations of α and β which results in a definite mismatch, amongst those, the one which α and β are changed equally gives the highest emittance increase, this is the used combination.

Halo value increases dramatically by increasing the mismatch value, for the three mismatch values of 10, 30, and 50% the average halo increase in three planes is 0.44, 1.92, and 2.74, while for a matched beam this value is 0.31, for the Gaussian beam truncated at $3 \times \sigma$.

CONCLUSION

The beam dynamics study of the nominal ESS lattice showed no negative effects. As a quick and not necessarily robust method to measure the sensitivity of a structure against initial beam errors a series of initial mismatch was implemented and their effect on beam emittance was reported. A mismatch can cause an extra emittance and halo increase which rise very quickly with mismatch value. Another measure for the robustness of the LINAC is its acceptance to beam size ratio, this parameter was studied for all the three phase spaces, the longitudinal acceptance and beam size is plotted in Fig. 4.

Table 3: emittance evolution in the 2011 hybrid SC LINAC.

	$\Delta\epsilon_x^*$	$\Delta\epsilon_y$	$\Delta\epsilon_z$
First period of spokes	7.33 %	13.64 %	10.54 %
Spokes - First period‡	3.16 %	-2.17 %	-1.73 %
Low β	1.79 %	-1.17 %	3.32 %
High β	0.24 %	4.65 %	-0.36 %
SC LINAC - First period‡	5.25 %	1.18 %	1.17 %

$^*\Delta\epsilon = (\epsilon_f/\epsilon_i) - 1$

‡ emittance increase minus the emittance increase in the first period.

ACKNOWLEDGEMENTS

I would like to thank Romuald Duperrier, and Steve Peggs for the fruitful discussions and suggestions during the preparation of this paper.

REFERENCES

[1] "ESS Volume III Update: Technical report status", 2003, http://ess-scandinavia.eu/documents/VolIII.pdf.

[2] M. Eshraqi, ESS AD Technical Note, ESS/AD/0010, http://eval.esss.lu.se/DocDB/0000/000037/002/ESS\%20LINAC\%20Optimization.pdf.

[3] R. Duperrier, N. Pichoff, and D. Uriot, Phys. Rev. ST Accel. Beams, **10**, 084201, (2007).

[4] P. Pierini, "Analysis of gradients for proton linac", Gradients and Betas for ESS LINAC, Lund, September 2010, Sweden, http://indico.hep.lu.se//materialDisplay.py?contribId=2&materialId=slides&confId=1012.

[5] R. Duperrier, N. Pichoff and D. Uriot, Proc. International Conf. on Computational Science, Amsterdam, The Netherlands, 2002.

[6] M. Reiser, Part. Accel., **8**, 167, (1978).

[7] J. Struckmeier, M. Reiser, Part. Accel., **14**, 227, (1984).

[8] I. Hofmann, G. Franchetti, O. Boine-Frankenheim, J. Qiang, R. D. Ryne, Phys. Rev. ST. Accel. Beams, **6**, 024202 (2003).

[9] R. Duperrier, N. Pichoff and D. Uriot, Proc. International Conf. on Computational Science, Amsterdam, The Netherlands, 2002.